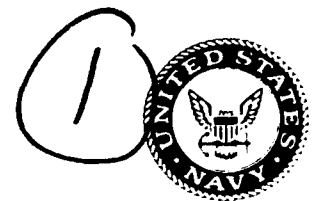


~~DTIC FILE COPY~~



Naval Research Laboratory
Washington, DC 20375-5000

NRL Memorandum Report 6703

DTIC FILE COPY

AD-A230 170

Coherent MM Wave Radar Using Incoherent Transmitter

DIETER R. LOHRMANN

*Ships EW Systems Branch
Tactical Electronic Warfare Division*

DTIC
ELECTE
SEP 05 1990
DEC 28 1990
S D CS D

August 21, 1990

90 12 27 001

~~90 05 00 000~~

REPORT DOCUMENTATION PAGE			Form Approved OMB No 0704-0188	
<small>Public reporting burden for this collection of information is estimated to average 1 hour per response, including the time for reviewing instructions, searching existing data sources, gathering and maintaining the data needed, and completing and reviewing the collection of information. Send comments regarding this burden estimate or any other aspect of this collection of information, including suggestions for reducing this burden, to Washington Headquarters Services, Directorate for Information Operations and Reports, 1215 Jefferson Davis Highway, Suite 1204, Arlington, VA 22202-4302, and to the Office of Management and Budget, Paperwork Reduction Project (0704-0188), Washington, DC 20503.</small>				
1. AGENCY USE ONLY (Leave blank)		2. REPORT DATE 1990 August 21		3. REPORT TYPE AND DATES COVERED
4. TITLE AND SUBTITLE Coherent MM Wave Radar Using Incoherent Transmitter			5. FUNDING NUMBERS	
6. AUTHOR(S) Dieter R. Lohrmann				
7. PERFORMING ORGANIZATION NAME(S) AND ADDRESS(ES) Naval Research Laboratory Washington, DC 20375-5000			8. PERFORMING ORGANIZATION REPORT NUMBER NRL Memorandum Report 6703	
9. SPONSORING/MONITORING AGENCY NAME(S) AND ADDRESS(ES) Naval Sea Systems Command Washington, DC 20361			10. SPONSORING/MONITORING AGENCY REPORT NUMBER	
11. SUPPLEMENTARY NOTES				
12a. DISTRIBUTION / AVAILABILITY STATEMENT Approved for public release; distribution unlimited.			12b. DISTRIBUTION CODE	
13. ABSTRACT (Maximum 200 words) A coherent MM wave radar using an incoherent transmitter is described. A breadboard of such a radar was constructed and successfully tested.				
14. SUBJECT TERMS			15. NUMBER OF PAGES 32	
			16. PRICE CODE	
17. SECURITY CLASSIFICATION OF REPORT UNCLASSIFIED	18. SECURITY CLASSIFICATION OF THIS PAGE UNCLASSIFIED	19. SECURITY CLASSIFICATION OF ABSTRACT UNCLASSIFIED	20. LIMITATION OF ABSTRACT UL	

CONTENTS

SUMMARY	1
1. INTRODUCTION	1
2. BASIC DESCRIPTION OF THE SCHEME	1
3. THE TEST SETUP	3
4. RESULTS	3
4.1 Discussion of Signals	3
4.2 Signal to Clutter Ratio	3
5. DESCRIPTION OF THE CIRCUITS	4
5.1 The E.I.O.	4
5.2 The HV Modulator for the E.I.O. Grid	4
5.3 The Phase Locked Local Oscillator (PLLO)	5
5.3.1 Measurement of Noise Spectrum of PLLO	6
5.4 Timing and Control Circuit	6
5.5 Phase Measuring and Shifting Circuit	6
5.6 Coherent Demodulator	7
5.7 EIO Frequency Control	7
5.8 Measurement of Peak to Clutter Ratio of Coherently Demodulated Signal Pulse	7
FIGURE CAPTIONS	8
DISTRIBUTION LIST	27



Accession For	
NTIS	CRA&I
DTIC	TAB
Unannounced	
Justified	
By	
Distribution /	
Availability Codes	
Dist	Avail and/or Special
A-1	

COHERENT MM WAVE RADAR USING INCOHERENT TRANSMITTER

O. Summary

A breadboard of a coherent mm wave radar using an incoherent transmitter was designed and tested. As transmitter was used an Extended Interaction Oscillator operating at 94 GHz with 1 kW pulse output power. The pulse peak to clutter ratio behind the synchronous detector was measured to be 26 dB for single pulse. It appears that this ratio was limited by phase noise performance in the receiver local oscillator and the target simulator and other circuitry rather than the EIO itself.

1. Introduction

A Microwave/ Millimeter Wave Dual Mode airborne missile simulator capability is going to be added to the present NRL Code 5740 simulator inventory.

The breadboard of the R.F. section of the mm wave radar for that Dual Mode is described in this preliminary report. It is unique in that it provides a coherent radar, using an incoherent R.F. transmitter.

It was decided to make the mm wave radar coherent in order to be able to simulate future threats even if these should use coherent radars. Furthermore, the radar could also be used for research in the mm wave range that requires a coherent radar. From the standpoint of the missile designer, using a radar emitting non - coherent pulses and still have the advantages of a coherent radar could be advantageous against ECM.

2. Basic description of the scheme.

The scheme of an IF Coherent Radar is not new. However, it appeared that the mm wave Extended Interaction Power Pulse Oscillator (EIO), due to its frequency stability, would work successfully with such a scheme. It is necessary that the phase within the r.f pulse is linear with time during the pulse, i.e., there is no chirp or random noise in the phase of the r. f. pulse. As our measurement shows, this is true to a large extent with the EIO we used in the setup described in this report.

The principle is this:

The r.f. phase in each r.f. pulse created by the r.f. pulse power oscillator is measured. The result is used to adjust the phase of a reference oscillator, such that when the signal

arrives from the target, it will be demodulated by this adjusted reference signal in a coherent fashion. For example, assume that one particular r.f. pulse has a phase that leads the phase of the reference oscillator by 35 electrical degrees. Then 35 electrical degrees are added to the phase of the reference oscillator right after the pulse was transmitted. The phase shift in the ref. oscillator stays until the next rf pulse is transmitted.

Fig. 1 shows the basic IF Coherent scheme:

EIO 1 creates 94 GHz pulses of 1 kW peak power, 300 ns duration and 8 kHz repetition rate. The pulses are r.f. incoherent, i.e., each r.f. pulse starts with a phase that is randomly distributed between zero and 360 deg.. Modulator 2 keys the EIO with the repetition rate of pulse generator 3. The r.f. pulse created by the EIO is transmitted thru circulator 4 and antenna 5 to the target 6. The return from target 6 enters the antenna and is then fed to the receiver mixer 5. Receiver mixer 5 receives its local oscillator signal from crystal controlled phase locked 93.86 GHz oscillator 17. The resulting I.F. constitutes incoherent pulses with 160 MHz center frequency. These are amplified in IF amplifier 7 and filtered in IF filter 8 in the conventional way. Coherent Demodulator 9 provides the Doppler output; the other input to the demodulator is the COHO signal. This COHO signal is derived as follows:

The transmitted pulse leaks thru circulator 4 to receiver mixer 5. At the output of receiver mixer 5 then appears a 160 MHz Xmit pulse. This pulse is sent to phase discriminators 10 and 11, where it is compared with the 160 MHz signal from Reference Oscillator 12. Between the reference oscillator and the phase discriminators is 90 deg Hybrid 13, such that at the output of discriminators 10 and 11 appear voltages proportional to the sine and the cosine of the difference angle. These voltages are fed to Sample & Hold circuits 14 and 15. The sampling pulse is coinciding with the transmit pulse; it is derived from the Rep. Rate pulse generator 3. The output voltages of S&H 14 and 15 represent the sine and the cosine of the phase difference between the r.f. pulses and the cw reference oscillator 12. These outputs are then fed to Phase Shifter 16, which adds the phase to the reference oscillator signal. Hence, the output of the Phase Shifter 16 is a 160 MHz signal with a phase that is adjusted to the phase of every transmitted r.f. pulse. Therefore, when the return pulse from the target arrives, it finds a COHO signal which has the proper phase for coherent demodulation.

3. The Test Setup

Fig. 2 shows the test setup block diagram. The path and the target are simulated by the Target Simulator Delay Repeater. It provides a 23 microsecond delay to simulate the return signal and a by-pass of the delay to provide the "leakage" of the Xmit pulse to the receiver mixer. The Doppler shift is simulated by insertion of pieces of 50 Ohm transmission line into the delay path with zero, lambda quarter and three quarter lambda electrical length.

Since the EIO had too much frequency drift during warm-up, (approx. 20 MHz), a frequency control loop was added to keep the center frequency of the EIO to 94 GHz \pm 100kHz.

The dc/dc converters in the high voltage sources were synchronized with an integer multiple of the Repetition Rate in order to prevent spurious modulations of the r.f. by the dc/dc converter ripples.

Fig. 3 shows a photo of the bench setup.

4. Results

4.1 Discussion of signals

Fig. 4 shows an oscillogram of the phase discriminator output. I output, which is proportional to $\sin(\phi)$ is deflecting horizontally, Q output (proportional to $\cos(\phi)$) is deflecting vertically. ϕ is the difference between the phase of the r.f. pulses of the E.I.O and the reference oscillator. The result is a circle, as should be.

Fig. 5 shows the output of the Phase Shifter with 50 kHz test signals at inputs I and Q. The signal at I leads that on Q by 90 degrees. The rf input was 160 MHz. Shown is the spectrum of the output signal at 160 MHz. Since the "Phase Shifter" is functionally the same as a Single Sideband Modulator, Fig. 5 shows the "carrier" down 33 dB and the suppressed (lower) "sideband" down 30 dB. In order to better designate its function, the Phase Shifter was not called a SSB modulator.

Fig. 6, 7 and 8 show the output of the signal pulse behind the Coherent Demodulator. In order to demonstrate the Doppler shift, zero, lambda quarter and 3/4 lambda long delay lines were added in the signal path, resulting in positive peak, zero and negative peak pulse output.

4.2 Signal to Clutter Ratio

The signal to clutter ratio of the signal output behind the coherent demodulator was measured by feeding the pulse to a Sample and Hold circuit. The clutter ratio CL is the ratio between the average peak amplitude of the pulse and the r.m.s of

the variation from that average. A true rms voltmeter was used to measure the variation, and a d.c. voltmeter to measure the average peak. The ratio measured was $CL = 26$ dB.

The delay was then adjusted to obtain zero average pulse output as in fig. 7. The ratio of average peak for max. output to the r.m.s deviation from zero average was 16 dB.

The clutter ratio of the E.I.O itself is probably better than 26 dB, because this was close to the limitation of the test set-up itself, primarily caused by the residual phase noise of the 94.3 and 93.84 GHz local oscillators and the accuracy of the phase adjustment circuits. This was verified by injecting a 300 MHz pulse derived from a HP 608 signal generator into the Target Simulator (see fig. 2) in lieu of the EIO derived transmit pulse. The clutter ratio measured for that case was 29 dB.

5. Description of the circuits

5.1. The E.I.O.

The E.I.O (Extended Interaction Oscillator) was the type VKB 2445S2 by Varian Canada. Its pulse output power is approx. 1 kW @ 94 GHz. It is keyed by a 3 kV pulse at the grid; its operational dc voltage on the cathode is -20 kV, the grid-cathode bias is -3 kV.

5.2 The HV modulator for the E.I.O. grid

Fig. 9 shows the schematic for the modulator. The drive pulse is fed to the cathode of the E.I.O. rather than the grid. Driving the grid instead does not considerably reduce the drive current requirement due to grid/cathode capacity, whereas driving the cathode permits elimination of the HV pulse transformer. In this scheme, the grid voltage is constant at -20kV, and during the pulse the cathode is driven negative by 3 kV from -17 kV to -20 kV by keying tube Q2 (8847A) on. Q2 and the transformer providing the 3 kV EIO grid bias, the EIO heater voltage and d.c. supply voltages for the grid of the driver tube and the pre-driver FET amplifier are located in an oil bath, further the H.V. capacitors.

Fig. 10 shows the high voltage d.c supplies, -17 kV for the cathode of the E.I.O. and 3.7 kV for the plate of the driver tube. The d.c. to HV converters are commercially available from Advanced HV Co.. Fig. 11 shows the driver circuitry of those converters by Advanced HV Co., with a custom synchronization circuit added by NRL. As mentioned above, the d.c. converters

were synchronized with a harmonic of the radar's repetition frequency in order to prevent ripple-induced jitter in the r.f. phase of the EIO. Further, Also, an input controlling the high voltage for tuning control of the E.I.O. was added. The tuning sensitivity was approx. 50 kHz /V . The input signal for this AFC is coming from the pulse r.f. discriminator, see fig. 2 and fig. 21.

Fig. 12 shows the connections of the EIO modulator.

5.3 The Phase Locked Local Oscillator (PLLO)

Fig. 13 shows the block diagram of the PLLO.

Gunn oscillator 4 provides a 93.84 GHz output.

A sample of this is mixed in Harmonic Mixer 6 with the tenth harmonic of 9.362 GHz source 7, resulting in a 220 MHz I.F.. The 9.362 GHz crystal controlled source 7 is commercially available from TCI, model # M5020 - 9362.

The I.F. is amplified by amplifier 8 and mixed with the 220 MHz signal from crystal oscillator 10 in phase discriminator 9.

The output of phase discriminator 9 controls the d.c. output of GUNN d.c. supply 3 via FET switch 13. Since the frequency of the GUNN oscillator depends on the d.c. supply level (typically 200 ... 300 MHz/V), the phase lock loop is closed.

The output from phase discriminator 9 is also sent to lock detector 12 thru low pass filter 11. Low pass filter 11 suppresses the 220 MHz leakage from phase discriminator 9.

GUNN Heater Control 16 keeps the GUNN oscillator at a temperature of 45 deg. C.

Lockup procedure:

After turn-on, switch 13 is open, opening the phase lock loop, until the Gunn oscillator reaches its proper temperature. This way, lockup to any wrong frequency during warm-up is prevented. Switch 2 is closed, feeding the signal from Saw Tooth Generator 1 to GUNN d.c. supply 3, thereby sweeping the GUNN oscillator by approx. 100 MHz at a rate of about once per second.

GUNN Heater Control 16 senses when the GUNN oscillator has reached its proper temperature and closes switch 13, thereby closing the phase lock loop. Lock detector 12 senses when lock condition occurs and opens switch 2, thus interrupting the sweep. Should phase lock be lost, Lock Detector 12 closes switch 2 again, thereby restarting the sweep.

The condition of switch 13 closed and switch 2 open is sensed by logic 14, signalling lock condition by lighting LED 15.

Isolator 5 separates the GUNN oscillator from the load.

Fig. 14 shows the schematic of the PLLO, fig. 15 its printed circuit board layout and fig. 16 the p.c. board mask.

5.3.1 Measurement of Noise Spectrum of PLL0

Since no source with better spectral purity was available, two almost identical such crystal controlled P.L.L. oscillators were mixed down to 460 MHz. Fig. 17 shows the resulting spectrum with 1 kHz resolution and fig. 18 with 100 kHz resolution. At 10 kHz off carrier, fig. 17 shows the noise to be 40 dB below carrier, corresponding to 70 dB in 1 Hz bandwidth. Assuming equal contributions of noise from each oscillator, its noise level is 73 dB below carrier in 1 Hz bandwidth. Integrated in a 3 MHz bandwidth, using fig. 17 and 18 for the graphical integration, the total noise is 29 dB below carrier.

5.4 Timing and Control Circuit

Fig. 19 shows the Timing and Control Circuit. It provides the transmit drive pulse, the receiver blanking pulse, the drive signals for the receiver protection switches and the receiver protection electronics and the transmitter VSWR detector and interlock.

5.5 Phase Measuring and Shifting Circuit, see fig.20, schematic.

The 160 MHz I.F. transmitter leakage pulse enters at point A. It is fed to a 90 deg. hybrid, whose two outputs feed two phase discriminators. The other input B of the phase discriminator comes from the 160 MHz reference oscillator; in the case of this bench setup, an HP 608D signal generator was used.

The outputs of the phase discriminators are entered into two fast Sample and Hold circuits; the sample pulse is derived from the transmit trigger pulse via monostable pulse generators 74LS123. Two 560 pF capacitors provide the "hold" function. Voltage droop during the repetition interval across these capacitors is a problem; a better solution would be a combination of an A to D converter with a S & H input, followed by a D/A converter. This would eliminate the droop and increase accuracy. Moreover, in a further improvement, the D/A converter and the Phase Shifter could be eliminated and the phase shift could be performed digitally in the Radar Data Processor Computer. The droop in the present design was quite small, none was visible on the scope. The sample function is performed by two FET's; one charges the holding capacitor during the transmit pulse, the other discharges it at the end of the repetition interval.

The I and Q signals appear at the output of the S&H circuit (points 1 and 2). These signals are fed into the Phase Shifter, consisting of two balanced mixers, which together with two operational amplifiers form four quadrant multipliers. The other input to the mixers is the 160 MHz reference signal B;

it is the same as the one mentioned above, just with a different level. Between the input of this ref. signal and the mixers is a 90 deg. hybrid, providing the necessary 90 degrees out of phase signal. Low pass filters at the output of the mixers eliminate higher harmonics of the 160 MHz signal; the outputs are then combined in a simple adder. The output D of this adder is the COHO signal used for coherent demodulation.

5.6 Coherent Demodulator

As coherent demodulator (see fig. 2) was used a MINICIRCUIT SBL-1 balanced modulator.

5.7 EIO Frequency Control

Fig. 21 shows the pulse r.f. frequency discriminator for the EIO AFC.

5.8 Measurement of Peak to Clutter Ratio of coherently demodulated signal pulse

As mentioned above, the peak to clutter ratio of the coherently demodulated pulse was measured by using a Sample and Hold circuit. The sampling signal was derived using a 100A Datapulse pulse generator, which was triggered by the transmit pulse and had a delay of 23 microseconds to match the delay in the repeater simulating the signal path (see fig. 2). Fig. 22 shows the S&H circuit used for the measurement.

FIGURE CAPTIONS

- Fig. 1: Coherent MM Wave Radar with Incoherent Transmitter, Block Diagram
- Fig. 2: Coherent MM Wave Radar with Incoherent Transmitter, Block Diagram of Test Setup
- Fig. 3: Breadboard of Test Setup
- Fig. 4: Phase Discriminator Output
- Fig. 5: Performance of Phase Shifter
- Fig. 6: Output of Coherent Modulator
- Fig. 7: Output of Coherent Modulator
- Fig. 8: Output of Coherent Modulator
- Fig. 9: Schematic of EIO Modulator
- Fig. 10: High Voltage DC Supplies
- Fig. 11: HV Supply by Advanced HV Corp. with Circuits Added by NRL
- Fig. 12: HV Modulator Connections
- Fig. 13: Receiver Phase Locked Local Oscillator (PLLO) Block Diagram
- Fig. 14: Receiver PLLO Schematic
- Fig. 15: PLLO Printed Circuit Board Layout
- Fig. 16: P.C. Board Mask for PLLO
- Fig. 17: Spectrum of PLLO, Mixing Down to 460 MHz with Second PLLO
- Fig. 18: Same as Fig. 14 but with Different Resolution
- Fig. 19: Radar Timing and Control Circuits
- Fig. 20: Phase Measuring and Phase Shifting Circuit Schematic
- Fig. 21: Schematic of Pulse R.F. Discriminator for EIO AFC
- Fig. 22: Sample and Hold Circuit for Peak to Clutter Measurement

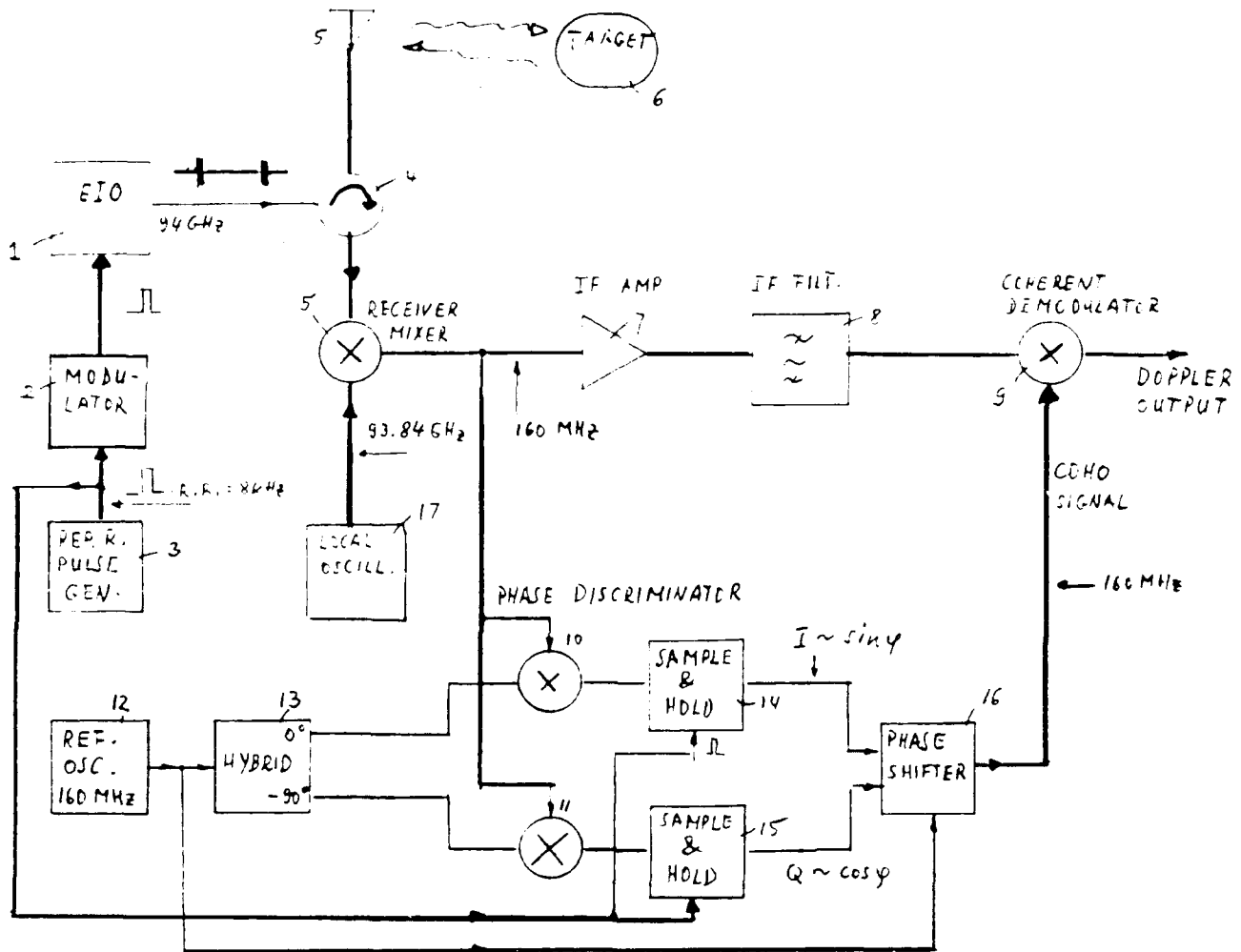


Fig. 1 — Coherent MM Wave Radar with Incoherent Transmitter

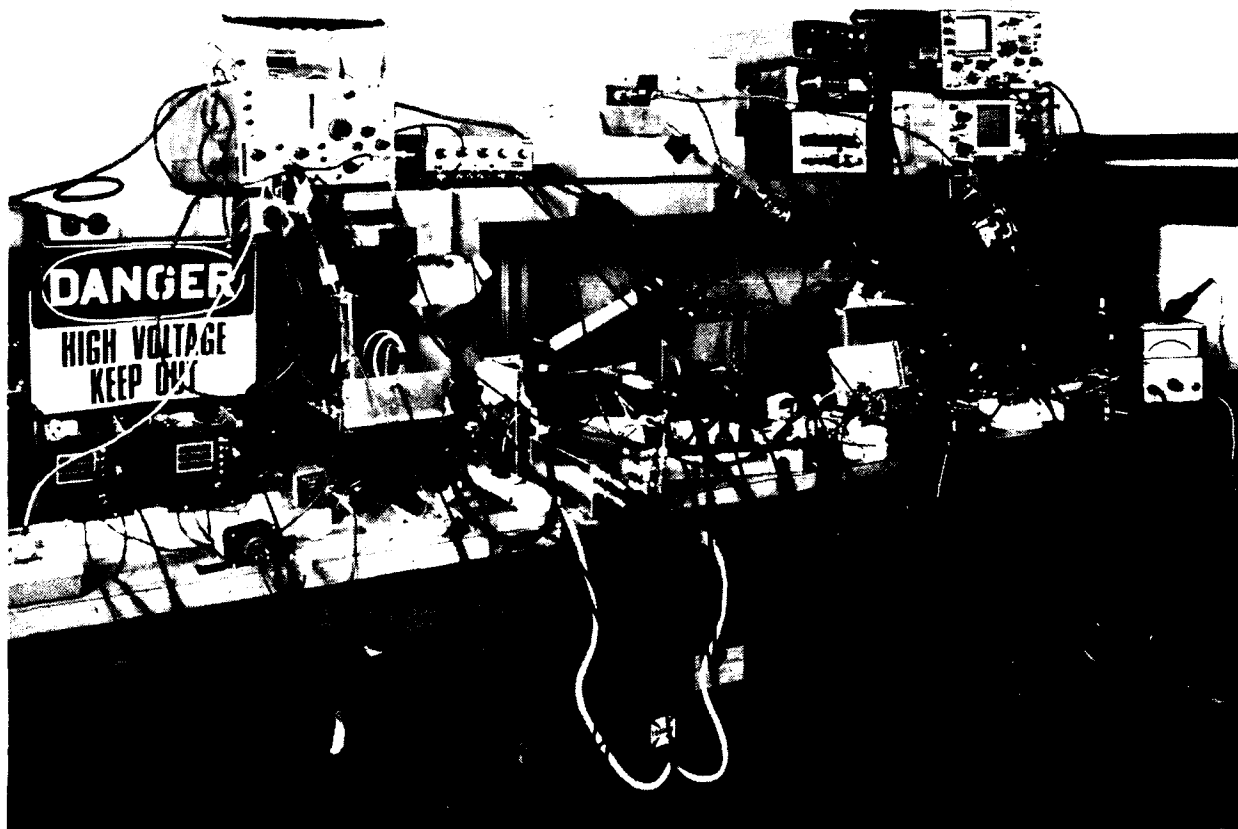


Fig. 3 -- Breadboard of Test Setup

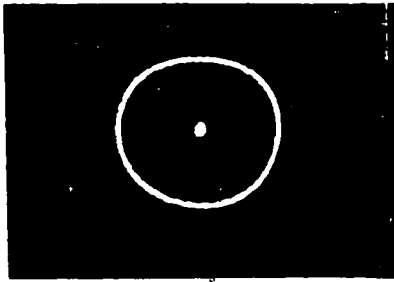


Fig. 4 -- Phase Discriminator Output

I is on X - Axis
Q is on Y - Axis

Hor: 1 V/Div.
Vert.: 1 V/Div.

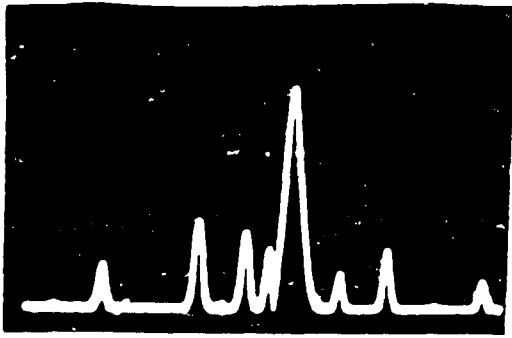


Fig. 5 — Testing the Phase Shifter

Input: Two 50 kHz signals with
90 deg. phase shift to
I and Q. I leads Q.
and 160 MHz c.w.

Output: Spectrum of 160 MHz signal
Hor.: 100 kHz/Div.
Vert.: 10 dB/Div.

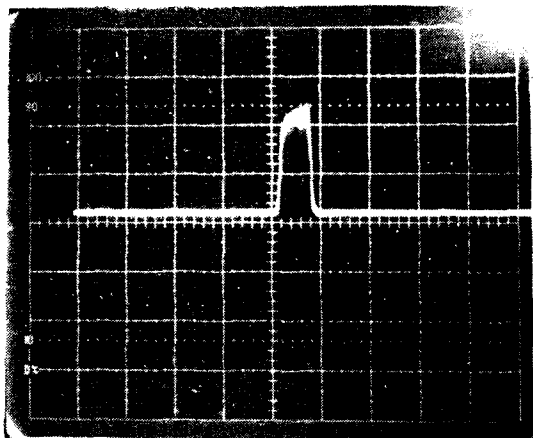


Fig. 6 — Output of Coherent Demodulator Signal Pulse has $23 \mu\text{s}$ Delay

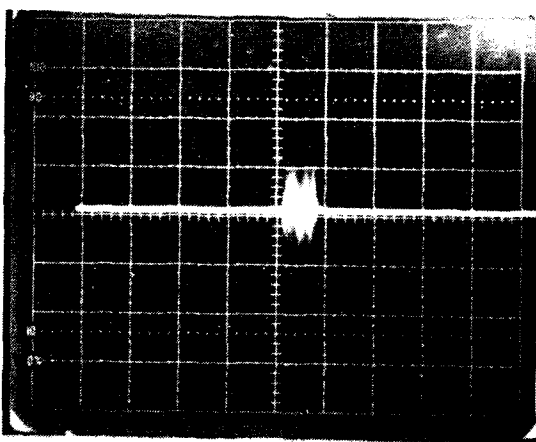


Fig. 7 — As Fig. 6, but with $\lambda/4$ delay added

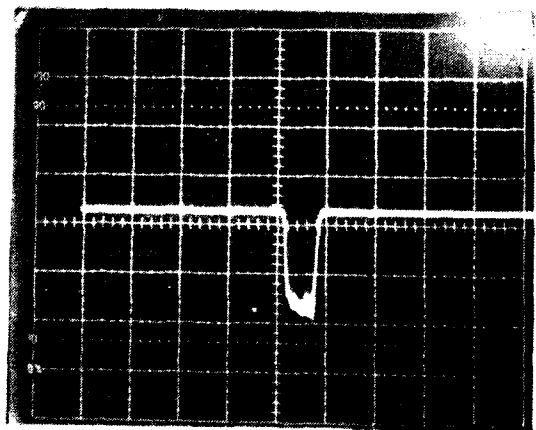


Fig. 8 — As Fig. 6, but with $3/4 \lambda$ delay added

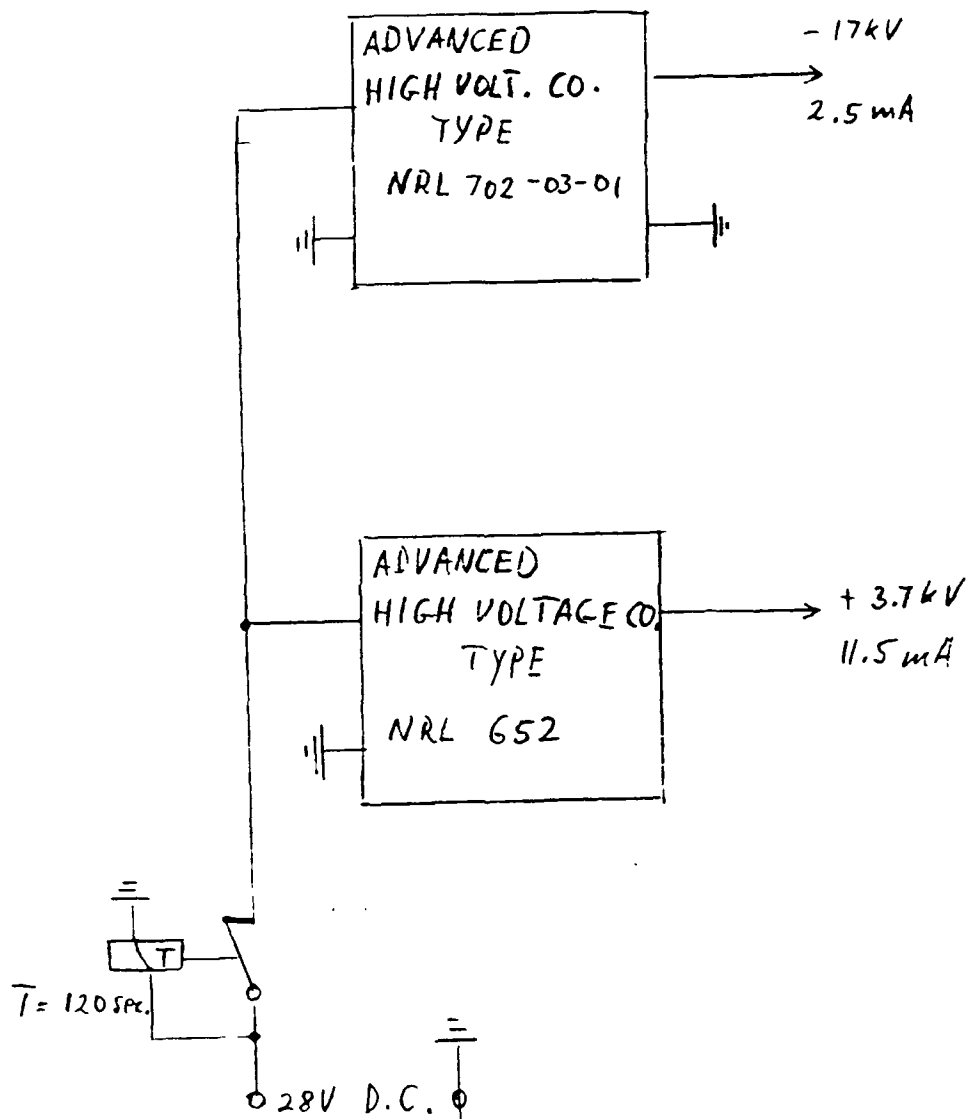


Fig. 10 — High Voltage D.C. Supplies

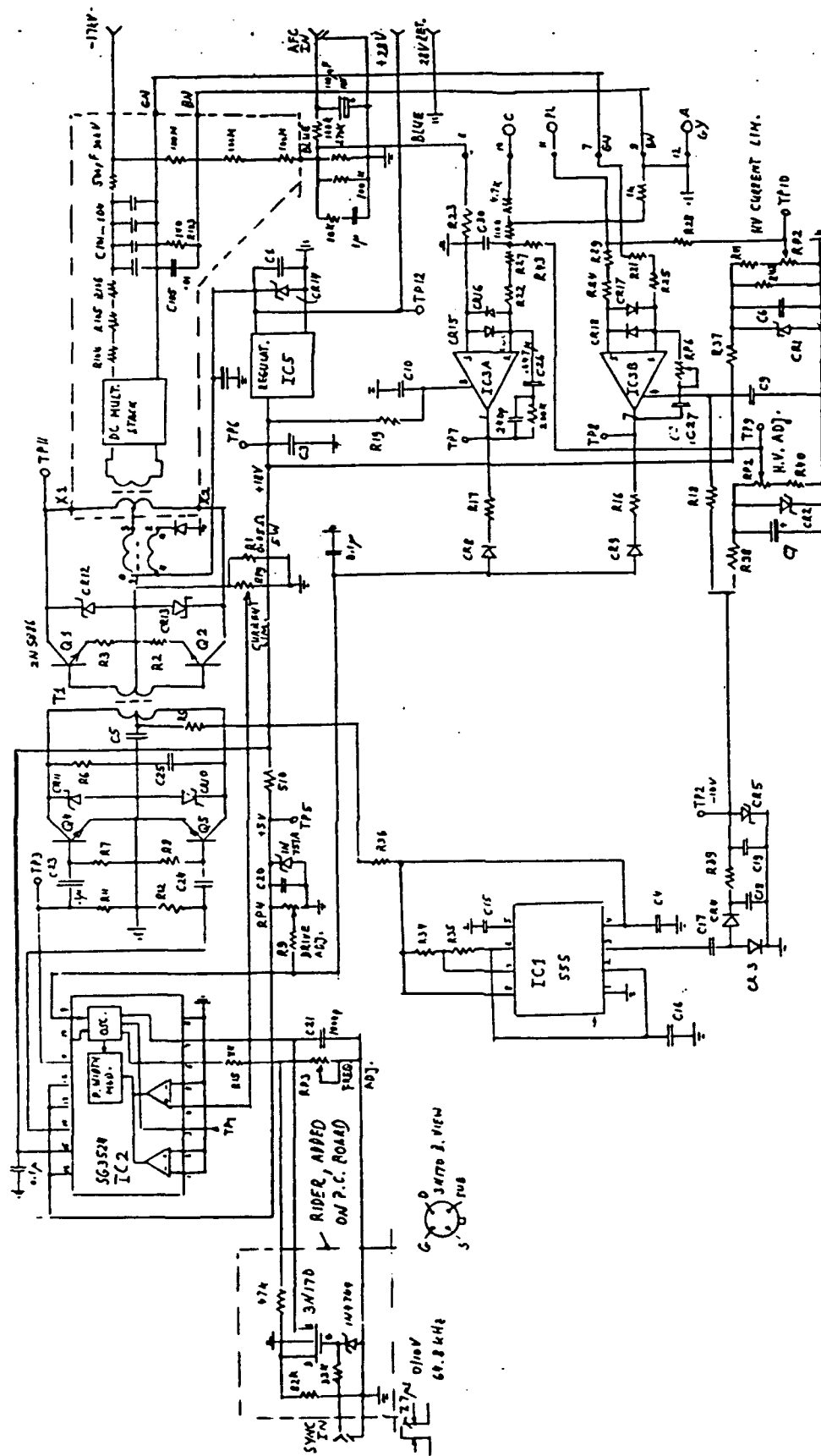


Fig. 11 — -17 kV HV Supply by Advanced High Voltage Corp. with Sync Circuit and AFC Input Added

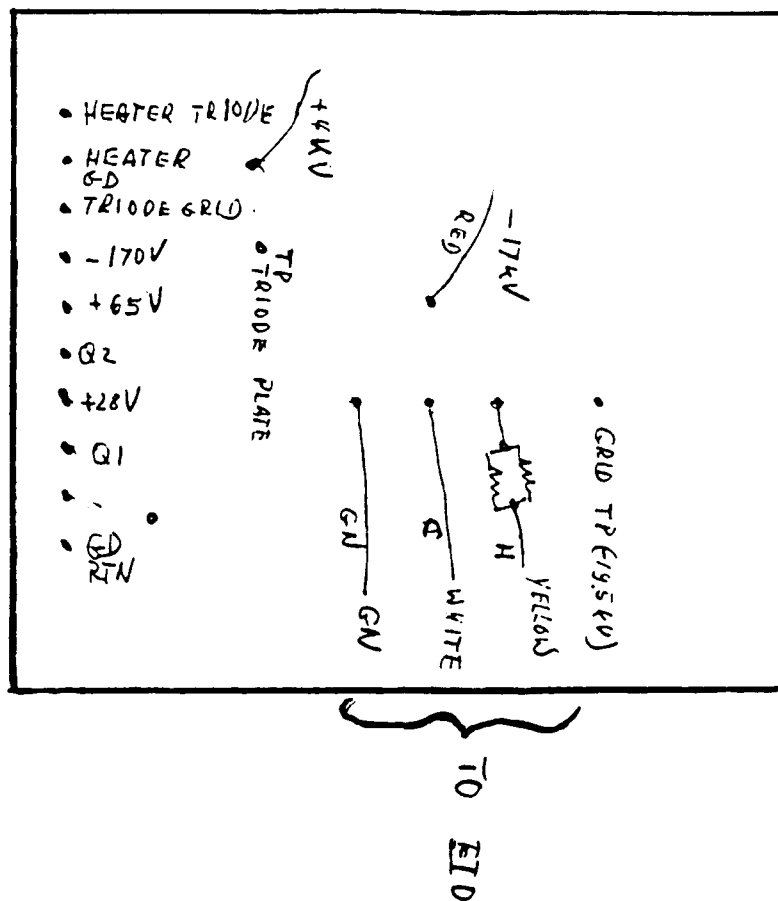


Fig. 12 — HV Modulator Connections

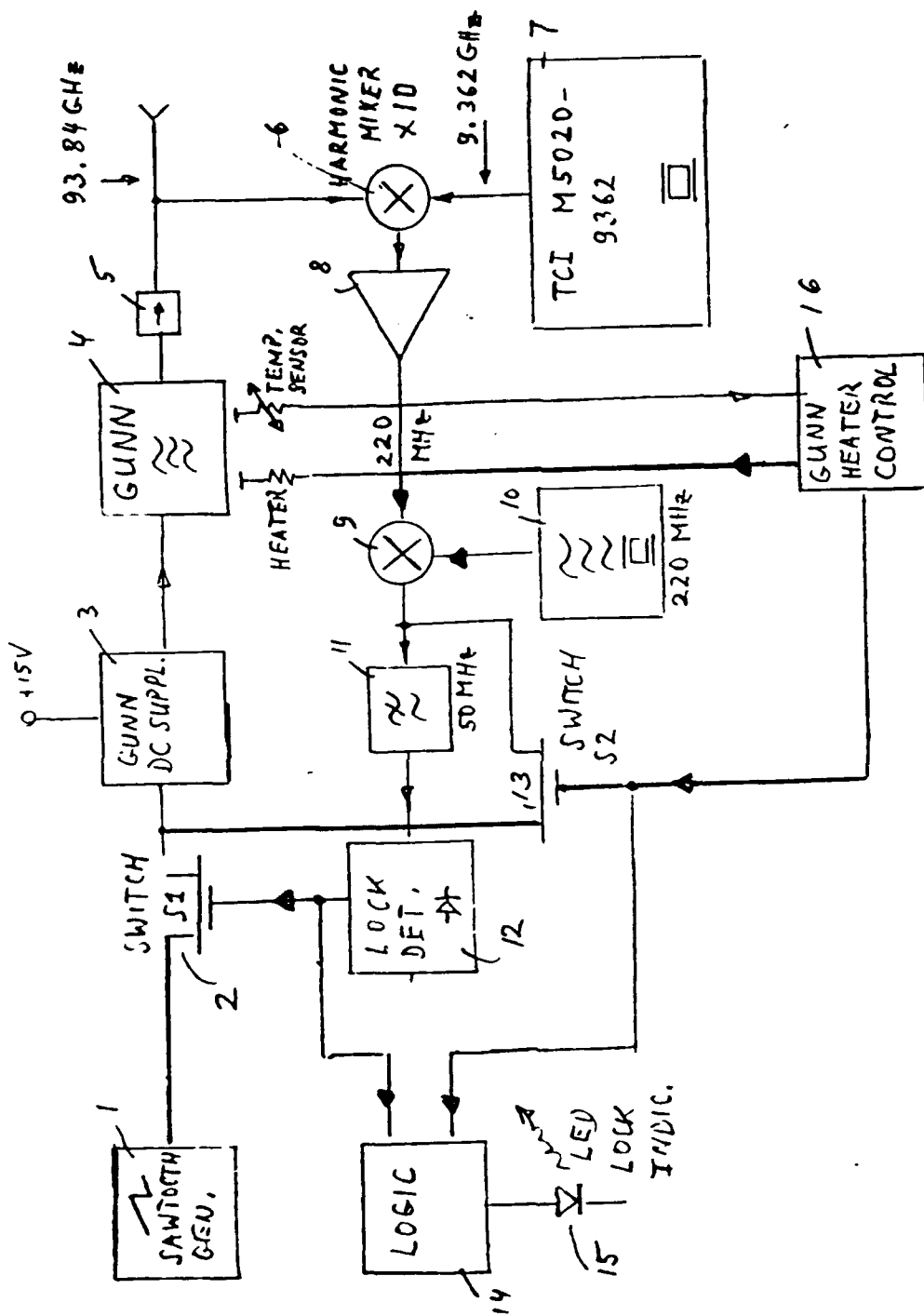


Fig. 13 — Block Diagram of PLLO



x2

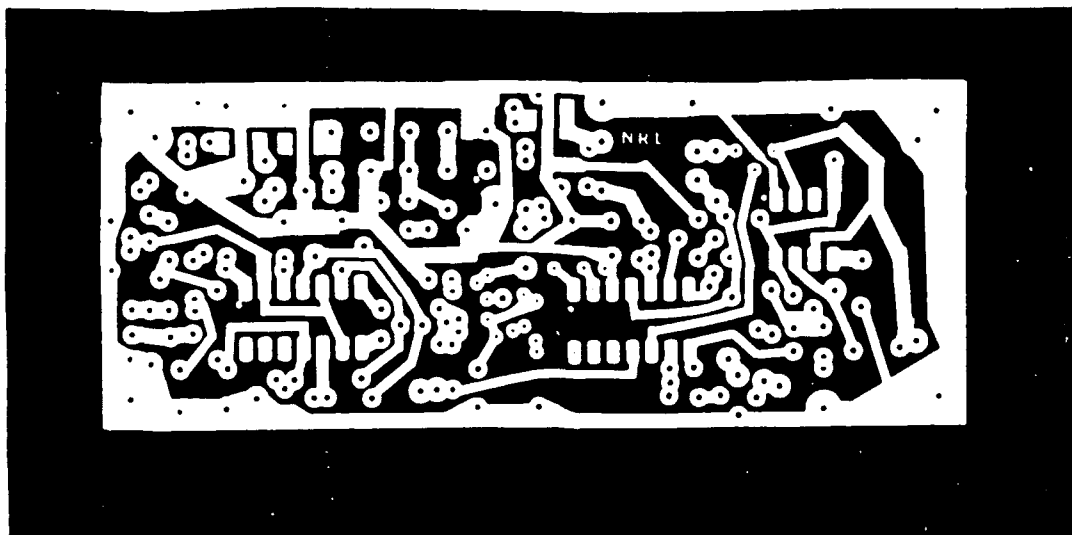


Fig. 16 — P.C. Board Mask for PLLO

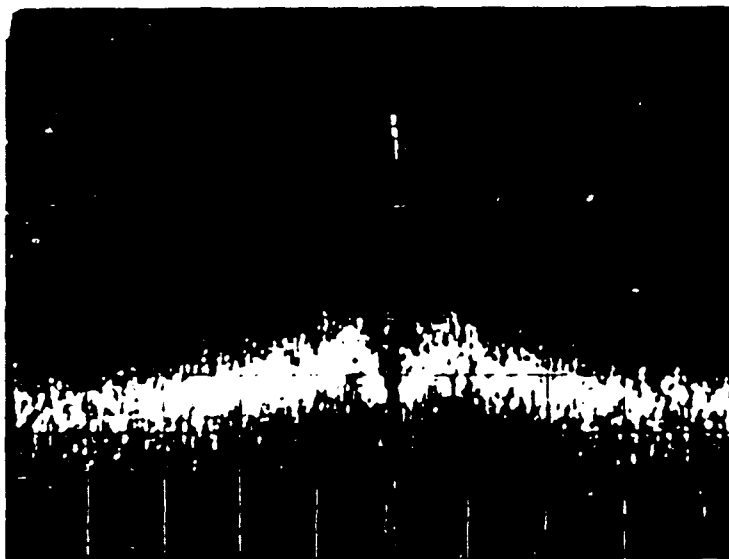


Fig. 17 — Spectrum for Two Crystal Controlled Phase Locked GUNN Oscillator Mixed Down to 460 MHz

Vert.: 10 dB/div.
 Hor.: 30 kHz/div.
 Resol. B.W. 1 kHz

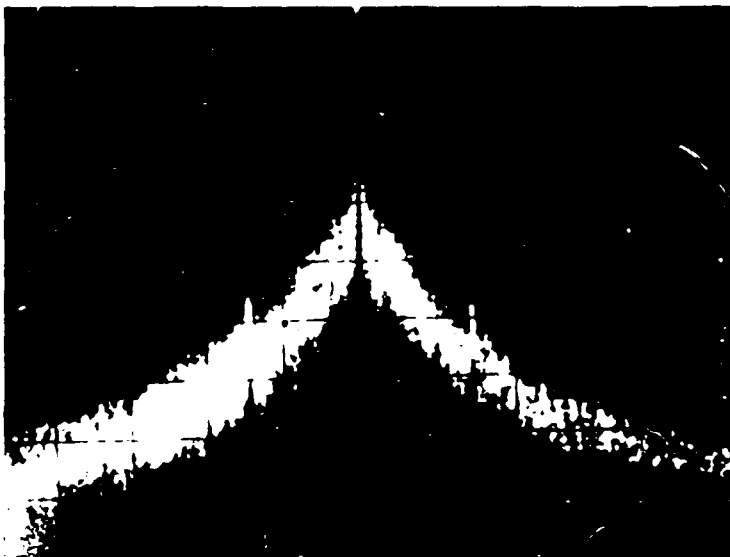
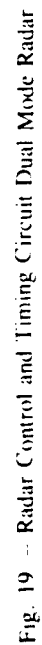
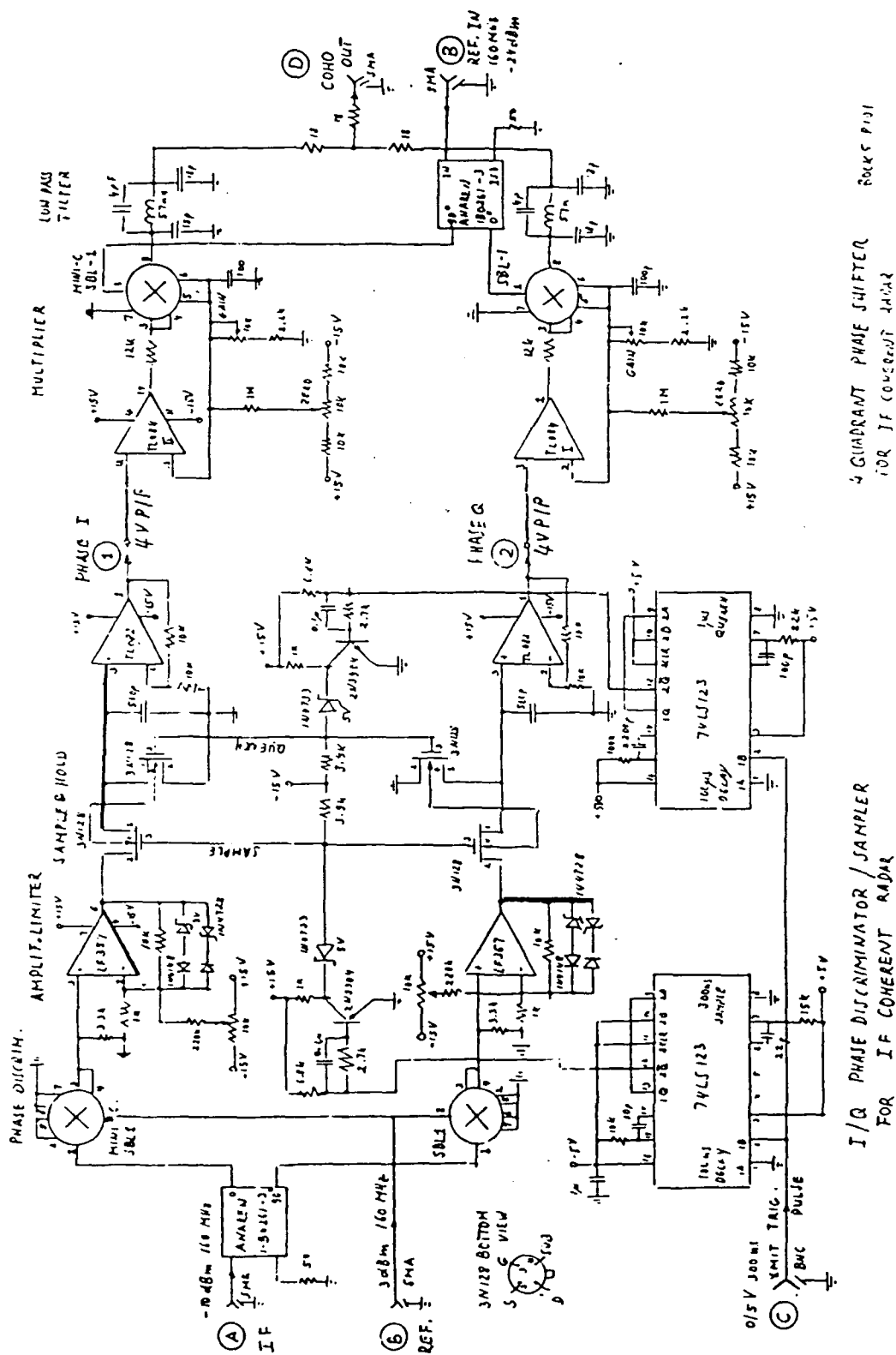


Fig. 18 — Same as Fig. 17
 Except Hor. = 3 MHz/div.
 Resol. B.W. = 100 kHz

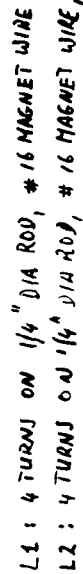




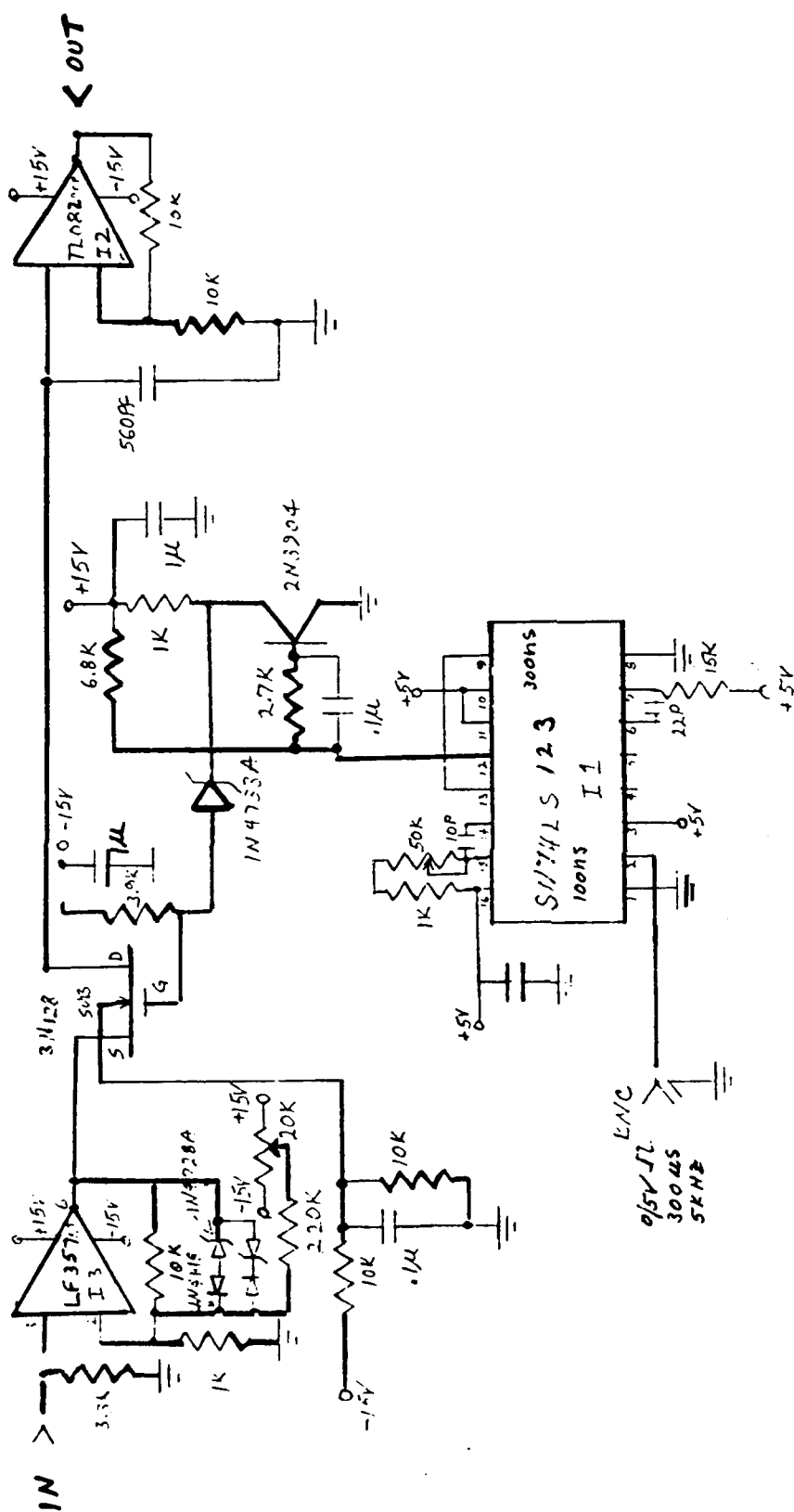
4 QUADRANT PHASE SHIFTER
FOR IF COHERENT RADAR

I/Q PHASE DISCRIMINATOR / SAMPLER
FOR IF COHERENT RADAR

Fig. 20 — Phase Measuring and Phase Shifting Circuit Schematic



25



DISTRIBUTION LIST
(MR6703)

Chief of Naval Research
800 N. Quincy Street
Arlington, VA 22217-5000
Attn: ONR-250, Program Manager of Surface Warfare
and Supporting Technologies
ONR-121D (LCDR T. R. Maynard)

Superintendent
U.S. Naval Post Graduate School
Monterey, CA 93940
Attn: Technical Librarian

Commander
Naval Surface Warfare Center
Danlgren, VA 22448-5000
Attn: Technical Librarian
Mr. Terry Reeder

Commanding Officer
Naval Ocean Systems Center
San Diego, CA 02152
Attn: NOSC, Code 7501 (Mr. Gerald M. Peake)
NOSC, Code 7502 (Mr. Robert Lawrence)
NOSC, Code 442 (Ms. Sue Hutchins)

Commanding Officer
Naval Avionics Center
6000 E. 21st Street
Indianapolis, IN 46219-2189
Attn: 072.5 (Mr. Don Lain)

Defense Technical Information Center (DTIC) (2 copies)

NRL Codes:	
2800	5720.02 (Mr. Leo Lemley)
4100	5730
4700	5740
4828 (20 copies)	5745.12 (20 copies)
5000	5750
5100	5800
5300	5900
5700	6100
5701	6300
5705	6500
5706	6800
5707 (ENEWS Library)	7500
5708	7700
5710	8100
5720	8120 (Mr. Joseph Koffley)

NRL Codes:

5325 (Dr. D. Himenway)
5733 (C. Hochuli)
8315 (B. Yaplee)
8315 (Commander G. Quick)
8311 (Dr. J. Hellinger)

Naval Research Laboratory
Washington, DC 20375-5000
(Code 4830)
Timothy Calderwood

Naval Technical Intelligence Center
4301 Suitland Road
Washington, DC 20395-5020
Attn: NTIC, Code DA-52 (Paul Hieschman)
NTIC, Code DA-44 (Mr. Mark Chapman/Mr. R.L. Brittingham)
NTIC, Code DE-00 (CAPT. Wickland)

Director
John Hopkins University
Applied Physics Laboartory
John Hopkins Road
Laurel, Maryland 20707
Attn: Code FP3 (Mr. Robert P. Borrelli)
Code NAS (Mr. Don J. O'Brien)
Mr. Dennis Serpico

Naval Air Development Center
Johnsvill
Warminster, PA 18974
Attn: NADC, Code 5023 (Mr. Sidney McCleary)

Commander
Space and Naval Warfare Systems Command
Washington, DC 20363-5100
Attn: SPAWAR 005R (Mr. Bernie DeSavage)
SPAWAR PMW-162-212 (LCDR A. B. Walter)
SPAWAR PMW-143-33 (CDR J. Campbell)

Director
Office of Naval Technology
800 N. Quincy Street
Arlington, VA 22217-5000
Attn: ONT, Code 215 (CDR Gary Quick)

Director of Research
U.S. Naval Acedemy
Annapolis, MD 21402
(2 copies)

Naval Research Laboratory
Washington, DC 20375-5000
(Code 1220)

Do NOT make labels for
Records----- (01 cy)